


 Cite this: *Lab Chip*, 2015, 15, 3905

Steering liquid metal flow in microchannels using low voltages†

 Shi-Yang Tang,^a Yiliang Lin,^b Ishan D. Joshipura,^b Khashayar Khoshmanesh^{*a} and Michael D. Dickey^{*b}

Liquid metals based on gallium, such as eutectic gallium indium (EGaIn) and Galinstan, have been integrated as static components in microfluidic systems for a wide range of applications including soft electrodes, pumps, and stretchable electronics. However, there is also a possibility to continuously pump liquid metal into microchannels to create shape reconfigurable metallic structures. Enabling this concept necessitates a simple method to control dynamically the path the metal takes through branched microchannels with multiple outlets. This paper demonstrates a novel method for controlling the directional flow of EGaIn liquid metal in complex microfluidic networks by simply applying a low voltage to the metal. According to the polarity of the voltage applied between the inlet and an outlet, two distinct mechanisms can occur. The voltage can lower the interfacial tension of the metal *via* electrocapillarity to facilitate the flow of the metal towards outlets containing counter electrodes. Alternatively, the voltage can drive surface oxidation of the metal to form a mechanical impediment that redirects the movement of the metal towards alternative pathways. Thus, the method can be employed like a ‘valve’ to direct the pathway chosen by the metal without mechanical moving parts. The paper elucidates the operating mechanisms of this valving system and demonstrates proof-of-concept control over the flow of liquid metal towards single or multiple directions simultaneously. This method provides a simple route to direct the flow of liquid metal for applications in microfluidics, optics, electronics, and microelectromechanical systems.

 Received 28th June 2015,
Accepted 6th August 2015

DOI: 10.1039/c5lc00742a

www.rsc.org/loc

Introduction

Liquid metal alloys such as eutectic GaIn (75% gallium and 25% indium)¹ and Galinstan (68.5% gallium, 21.5% indium, and 10% tin)² possess many remarkable properties such as high electrical and thermal conductivities, high surface tension, extremely low vapour pressure, melting points below room temperature, and most importantly low toxicity in comparison to mercury.² Due to these remarkable properties, gallium based liquid metals have been integrated into microfluidic systems for pumping,^{3,4} mixing,^{5,6} enhancing convective heat transfer,⁷ making electronic circuits such as antennas,^{8–10} electronic filters¹¹ and sensors,^{12–14} as well as forming microelectrodes for stimulating neural cells¹⁵ and trapping nanoparticles using dielectrophoresis⁷ in microfluidics.

In the aforementioned applications, the liquid metal components are effectively static. However, there is also a possibility to create dynamic structures within microfluidic systems

based on continuous flow of liquid metal for conducting electrical current (*e.g.*, for switches, electrodes, wires, or reconfigurable antennas), dissipating heat, or patterning liquid metal at desired locations. Controlling the direction liquid metal flows at branching points in microchannels is important for achieving such shape reconfigurable metals in microfluidic systems. One approach could be to pump the metal and utilize microvalves to direct the flow along desired paths. Microvalves using either mechanical movable membranes powered by magnetic,¹⁶ electric,¹⁷ piezoelectric,¹⁸ pneumatic¹⁹ and thermal²⁰ mechanisms, or moving parts activated by phenomenon such as bistability,²¹ electrochemistry²² and phase change²³ have the potential to be implemented in microfluidic systems for controlling the flow of liquid metal. However, all these systems are based on moving parts, which have several drawbacks such as the potential for failure and rather complicated fabrication processes.²⁴ As such, developing a method for controlling the directional flow of liquid metal with no moving parts and easy implementation is appealing.

In this work, we demonstrate and characterize a novel method for controlling the directional flow of liquid metal in complex microfluidic networks simply by applying a modest voltage. Here, we define ‘complex’ microchannels as those

^a School of Electrical and Computer Engineering, RMIT University, Melbourne, Australia. E-mail: khashayar.khoshmanesh@rmit.edu.au

^b Department of Chemical and Biomolecular Engineering, North Carolina State University, USA. E-mail: mddickey@ncsu.edu

† Electronic supplementary information (ESI) available. See DOI: 10.1039/c5lc00742a

with at least one branching point such that the liquid metal has two or more unique paths through which it can flow. The application of voltage to the metal changes the interfacial properties of the metal at its leading end. According to the polarity of the voltage, the interfacial tension of the metal can be lowered to facilitate its movement towards a desired outlet by means of electrocapillarity (*i.e.*, continuous electro-wetting, CEW), or the surface of the metal can be oxidized, lowering its fluidity and directing the metal towards alternative outlets. Both methods enable ‘valving’ to direct the movement of the metal without mechanical moving parts. In addition to directing the metal along desired paths, the use of voltage can also retract the metal from undesired paths. Voltage has been used previously to spread droplets of liquid metal and direct the movement of the liquid metal within capillary tubes and open-top channels at mm length scales.²⁵ This paper describes the use of voltage to direct the continuous flow of liquid metal along unique pathways through sealed, complex microchannels. We investigate the mechanisms underlying the operation of this valving system and conduct proof-of-concept experiments to show the capability of this method for controlling the flow of liquid metal towards single or multiple directions simultaneously.

Materials and methods

Experimental setup

Fig. 1A is a schematic of the experimental setup. We used standard soft lithography techniques²⁶ to fabricate a T-shaped microchannel composed of polydimethylsiloxane (PDMS) with a width and height of 1000 and 75 μm , respectively, and bonded it onto a glass slide after treatment with an oxygen plasma. After prefilling the microchannel and the outlet reservoirs with 1 M NaOH solution, we injected eutectic gallium indium liquid metal (EGaIn, 75 wt% gallium and 25 wt% indium, Indium Corporation) through the inlet using a syringe pump (Fusion 100, Chemyx). Fig. 1B shows the experimental setup, in which the liquid metal flows through a stainless steel tube inserted into the inlet of the microchannel to provide electrical contact.

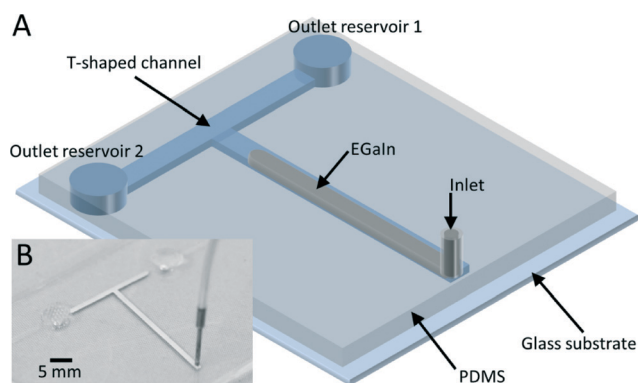


Fig. 1 Experimental setup. A schematic of the experimental setup is given in (A) and a photograph of the actual image for the setup is given in (B).

Video capture

A digital single lens reflex camera (Nikon D800) fitted with a macro lens (Sigma 105 mm F2.8 Macro) captured videos of the metal in the microchannel. A high-speed camera (Phantom v4.2, Vision Research Inc.) fitted onto an inverted microscope (Olympus, GX71) captured video at higher frame rates when necessary.

Results and discussion

We utilized a syringe pump to inject liquid metal continuously into the microchannel at a flow rate of 40 $\mu\text{L min}^{-1}$. In the absence of potential, the metal flows from the inlet to the ‘T-junction’ at which point the flow splits evenly between the two outlet pathways, as expected. Fig. 1B shows a snap-shot from this control experiment taken before the metal reaches the outlet. Once the metal reaches the outlet, it forms droplets as it exits into the reservoir holding the electrolyte.

Applying a negative (cathodic) potential to the metal relative to a counter electrode removes the oxide layer that forms on the metal, which influences the flow of the metal. We connected the cathode to the stainless steel tube inserted into the inlet port and connected one of the outlet reservoirs to the anode using a copper wire, as shown in Fig. 2A. This electrode arrangement creates asymmetry since the electrical path traces only from the inlet to Outlet 1 (defined arbitrarily as the outlet on the right in Fig. 2). Applying 0.5 V DC causes the flow of liquid metal to gradually re-direct towards Outlet 1, as shown in Fig. 2B and C. The current measured in this case is $51 \pm 3 \mu\text{A}$, resulting in a power consumption of $25.5 \pm 1.5 \mu\text{W}$. Similarly, the liquid metal switches direction by applying the DC voltage to Outlet 2, as shown in Fig. 2D–F. Movie S1† shows the process of directing and redirecting the flow of liquid metal. Liquid metal microdroplets form at the outlet due to sudden expansion as the metal exits the channel into the outlet reservoirs. The frequency of droplet formation increases in response to the DC voltage, as shown in ESI† S1 and Movie S2.

The application of a cathodic potential to the metal has two notable effects. First, it lowers the interfacial tension of the metal,²⁵ which causes the metal to flow preferably along the path that leads toward the counter electrode (*i.e.*, along the path of lowest surface tension). The higher interfacial tension of the metal along the other pathway causes the metal to withdraw toward the counter electrode until eventually all the metal flows along the electrical path (*i.e.*, toward the counter electrode). Second, the applied potential creates a gradient of surface tension along the surface of the liquid metal. Fig. 2G shows the equivalent circuit for one of the outlets. A narrow slip layer separates the liquid metal from the channel walls so that the solution completely surrounds the liquid metal.²⁷ R_{solution} and R_{SL} represent the resistance of the NaOH solution in the reservoir and along the slip layer between the liquid metal and the channel wall along the microchannel, respectively. The equivalent circuit of the electrical double layer (EDL) formed on the surface of liquid

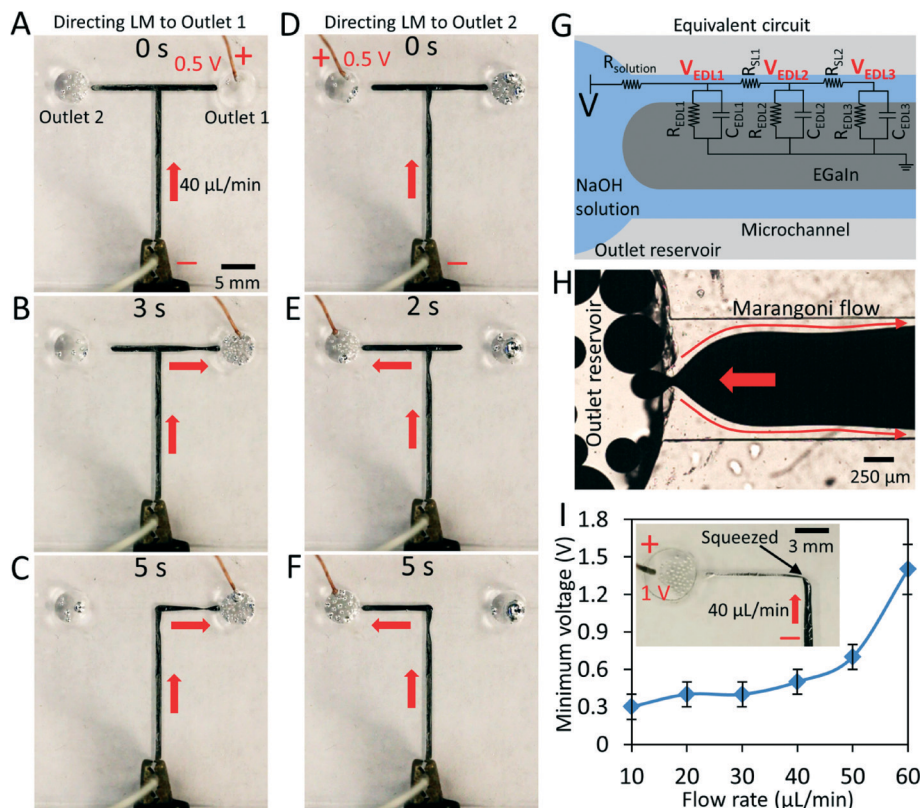


Fig. 2 Directing the flow of liquid metal using electrocapillarity. Sequential snapshots that show the flow of liquid metal directing towards (A–C) Outlet 1 and (D–F) Outlet 2, upon application of 0.5 V DC. The liquid metal is the cathode. (G) Equivalent circuit for liquid metal and surrounding NaOH solution. (H) Trajectory of the induced Marangoni flow when a voltage is applied. (I) Plot for the minimum voltage required for directing the flow of liquid metal vs. flow rate of liquid metal, the inset shows the squeezing of liquid metal when the applied voltage is larger than the minimum voltage required.

metal can be represented using a charge-transfer resistance R_{EDL} in parallel with an EDL capacitance C_{EDL} . When a DC voltage is applied, the voltage drop across the EDL (V_{EDL}) is larger at the side closer to the outlet reservoir ($V_{\text{EDL1}} > V_{\text{EDL2}} > V_{\text{EDL3}}$) since there is a voltage drop along the slip layer due to resistance R_{SL1} and R_{SL2} .

Interfacial tension between the liquid metal and the solution depends on V_{EDL} , as described by Lippman's equation,²⁸

$$\gamma = \gamma_0 - \frac{1}{2} C_{\text{EDL}} V_{\text{EDL}}^2 \quad (1)$$

where γ is the interfacial tension and γ_0 is the maximum interfacial tension when $V_{\text{EDL}} = 0$. Thus, the interfacial tension of liquid metal is smaller on the side closer to the outlet reservoir. This interfacial tension gradient generates Marangoni flow along the surface of liquid metal, as shown in Fig. 2H. The induced Marangoni flow acts as a 'conveyor belt' and transfers the surrounding NaOH solution into the microchannel, increasing the thickness of the slip layer and meanwhile pulling the liquid metal itself towards the outlet reservoir. This phenomenon is also called CEW.²⁹ The addition of 10 μm polystyrene microparticles into the NaOH

solution helps visualize the trajectory of the Marangoni flow, as clearly shown in the high-speed Movie S3.†

We investigated the minimum voltage required for directing the flow of liquid metal to the selected outlet reservoir as a function of flow rate. We varied the flow rate of liquid metal from 10 to 60 $\mu\text{L min}^{-1}$ in steps of 10 $\mu\text{L min}^{-1}$ and recorded the minimum voltage required for directing the liquid metal, as shown in Fig. 2I. Directing the flow of liquid metal at higher flow rates necessitates larger voltages. Consequently, the current and power necessary for steering the metal also increase with flow rate. For example, the current increases from 31 ± 6 to 143 ± 18 μA when the flow rate of liquid metal increases from 10 to 60 $\mu\text{L min}^{-1}$. To estimate the flow rate of the liquid metal exiting the desired outlet we measured the size and frequency of the emerging droplets. For a flow rate of 40 $\mu\text{L min}^{-1}$ injected into the inlet, increasing the voltage from 0 to 0.5 V increases the flow rate at the exit of the microchannel from 23 ± 4 to 47 ± 6 $\mu\text{L min}^{-1}$. The doubling of flow rate corresponds to fully directing the liquid metal flow towards the desired outlet reservoir. However, increasing the voltage further to 1 V induces temporarily a higher flow rate of 160 ± 8 $\mu\text{L min}^{-1}$ at the exit of the microchannel, indicating that CEW squeezes the liquid metal toward the outlet reservoir faster than the injection of the

liquid metal. As a result, the metal is not able to fill the entire channel, as shown in the inset of Fig. 2I, and the flow of the metal is not stable.

The experiments reported in Fig. 2 indicate the ability to electrically control the flow of liquid metal, similar to a valve but without any mechanical parts. Based on this principle, it is possible to direct the flow of liquid metal towards multiple outlets sequentially or simultaneously. As a demonstration, we created a cascade of T-junction channels with eight outlets, as detailed in ESI† S3.

After prefilling the microchannel and the outlet reservoirs with 1 M NaOH solution, a syringe pump injected the liquid metal at $40 \mu\text{L min}^{-1}$. Fig. 3A and B show that a 7 V DC signal directs the metal towards the outlet reservoir containing the anode. Moving the anode into different reservoirs changes the pathway through which the metal moves (see Movie S4†). The use of longer microchannels necessitates the use of a larger voltage (7 V vs. 0.5 V). The flow of the liquid metal is not continuous since the liquid metal pinches off in the microchannel due to the strong CEW effect induced by the large applied voltage. As such, the current is unstable and ranges from 140 to 1010 μA . However, applying a smaller voltage leads to the leakage of liquid metal towards other undesired outlet reservoirs.

Additionally, it is possible to direct the flow of liquid metal towards multiple outlets simultaneously by applying the voltage to the selected outlet reservoirs, as given in Fig. 3C–D and 3E–F in which the flow of liquid metal directs into two and three selected outlets, respectively (also see Movie S4†).

It is also possible to control the direction of the flow of liquid metal by switching the polarity of the electrodes. The application of a positive (oxidative) bias to the metal drives the formation of an oxide layer on the metal and provides a mechanism to direct flow without harnessing the CEW effect. Fig. 4A shows the response of the metal by applying a +5 V

DC signal to the inlet relative to a counter electrode placed in Outlet 1, while injecting liquid metal at $40 \mu\text{L min}^{-1}$. In this case, liquid metal flows towards both outlet reservoirs initially, as shown in Fig. 4B. However, the flow towards the Outlet 1 eventually stops after ~ 5 s and liquid metal only flows towards Outlet 2, as shown in Fig. 4C. In this case, the current is ~ 1.03 mA, resulting in a power consumption of ~ 5.15 mW. A similar phenomenon occurs when placing the cathode in Outlet 2, in which case liquid metal only flows towards Outlet 1 (Fig. 4D–F). Movie S5† shows the process for directing the flow of liquid metal using oxidative potentials.

The application of a positive potential to the metal drives the oxidation of the metal. The formation of oxide on the surface lowers the surface tension of the metal, but also creates a mechanical impediment to flow. A similar approach has been reported to block the flow of Galinstan liquid metal within a microchannel.³⁰ The presence of NaOH removes the oxide layer and competes with the electrochemical deposition of the oxide layer. The rate of deposition increases as the metal approaches the counter electrode due to the lowered resistance through the circuit (as metal displaces electrolyte). Consistent with this reasoning, Movie S5† suggests that the metal flows toward both outlets until the mechanical barrier provided by the oxide prevents further progress of the metal toward the outlet. As the metal approaches the outlet, it has a concave meniscus, as expected (Fig. 4G). Surprisingly, it inverts to a convex meniscus as it approaches the cathode, as shown in Fig. 4F. As the liquid metal approaches the cathode, the liquid metal at the center of the microchannel presumably oxidizes faster since this part is closer to the cathode (Fig. 4G). As a result, the liquid metal closer to the sidewalls moves faster than the metal at the center of the channel (Fig. 4H). Eventually, the solid oxide layer grows thick enough to stop the flow of liquid metal moving towards the outlet, forming a receding meniscus at the edge of oxidized liquid

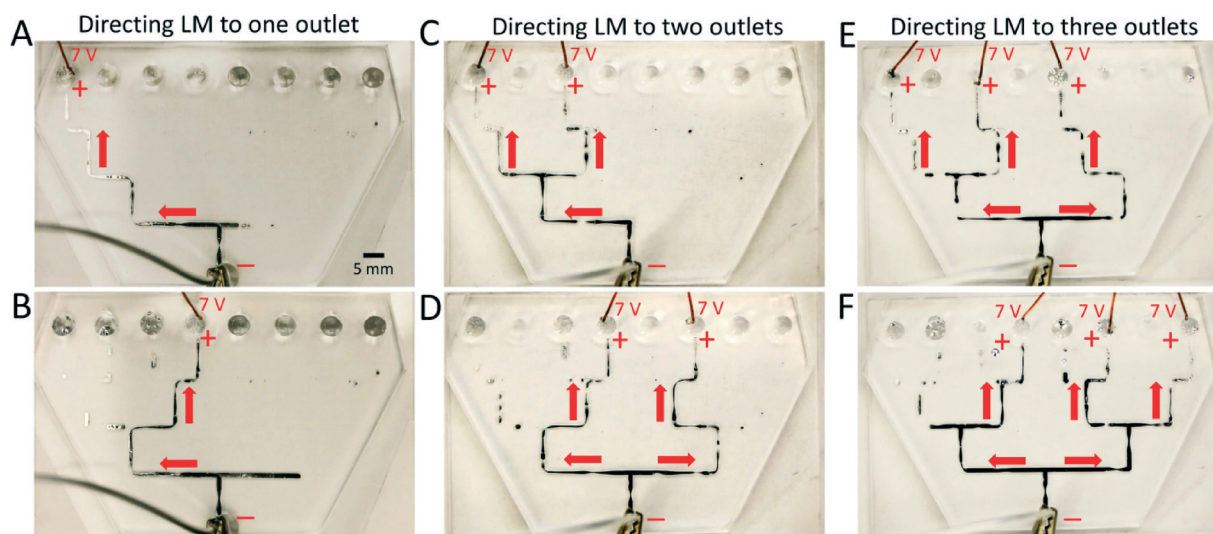


Fig. 3 Directing the flow of liquid metal towards (A–B) one, (C–D) two, and (E–F) three outlets using voltage. Liquid metal is injected at $40 \mu\text{L min}^{-1}$ for all cases.

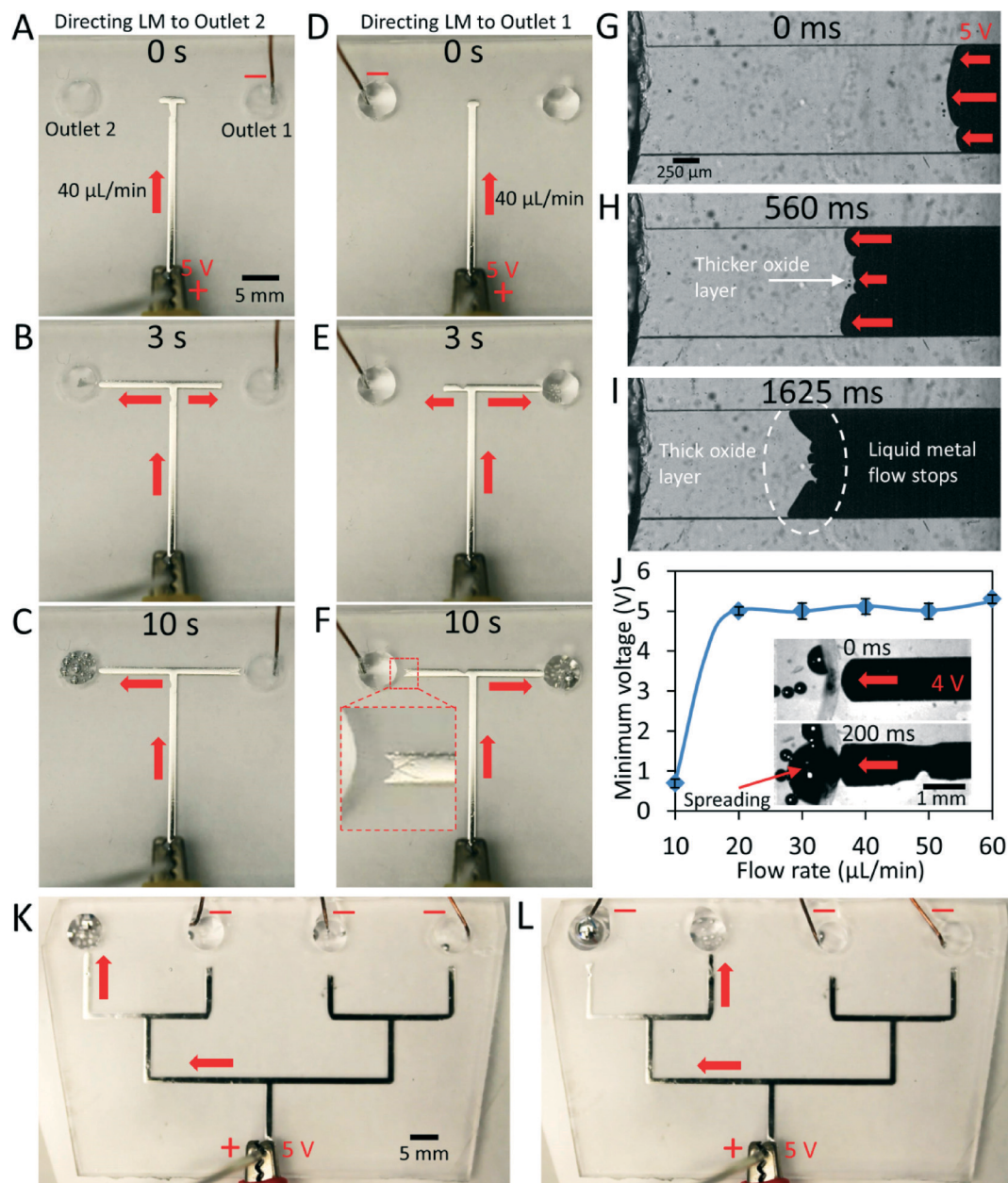


Fig. 4 Directing the flow of liquid metal towards the opposite reservoir. Sequential snapshots for directing the flow of liquid metal towards (A–C) Outlet 2 and (D–F) Outlet 1, when applying 5 V DC voltage. The liquid metal is connected to the anode. (G–I) Sequential snapshots for the microchannel close to Outlet 2, demonstrating the procedure for stopping the liquid metal flow and the formation of a receding meniscus at the edge of oxidized liquid metal. (J) Plot for the minimum voltage required for directing the flow of liquid metal vs. flow rate of liquid metal. The inset shows the spreading of liquid metal towards the reservoir when the applied voltage is smaller than the minimum voltage required for directing flow. (K–L) Directing liquid metal towards one outlet by placing the cathode in the rest of the reservoirs, a 5 V DC signal is applied and the flow rate of liquid metal is set to $40 \mu\text{L min}^{-1}$ opposite reservoir due to surface oxidation.

metal (Fig. 4I). Once the oxide is sufficiently thick, the liquid metal flow moves entirely toward the other outlet reservoir. In the absence of the electrochemical driving force, the base removes the oxide and allows the metal to start flowing again.

We investigated the minimum voltage required for directing the flow of liquid metal selectively toward a single outlet reservoir *versus* flow rate. Fig. 4J reports that halting the flow in one direction requires a minimum voltage of ~ 5 V at flow rates above $10 \mu\text{L min}^{-1}$. Applied voltages smaller

than the minimum value can cause the liquid metal to spread within the outlet reservoir that contains the counter electrode, as shown in the insets of Fig. 4J. The spreading is due to the lowered surface tension of the liquid metal arising from the formation of the oxide layer on the surface.²⁵ Liquid metal does not ‘leak’ to the other reservoir during the spreading process.

This method makes it possible to direct the flow of liquid metal in complex microchannels. For example, Fig. 4K and L

Table 1 Comparison between the electrocapillarity and surface oxidation methods for directing the flow of liquid metal

Method	Advantages	Disadvantages
Electrocapillarity	<ul style="list-style-type: none"> • Lower operating voltage • Lower power consumption • Faster response time • Can be used in both basic and neutral solutions 	<ul style="list-style-type: none"> • Pinch-off of liquid metal occurs
Surface oxidation	<ul style="list-style-type: none"> • Liquid metal can be patterned in microchannels • No pinch-off of liquid metal occurs 	<ul style="list-style-type: none"> • Higher operating voltage • Higher power consumption • Slower response time • Works best in basic solution

show that the liquid metal directs towards a desired outlet reservoir by placing the cathode in the rest of the other reservoirs in a cascaded, branched microfluidic channel.

Both surface oxidation and electrocapillarity can direct the flow of liquid metal in microchannels in a versatile manner. Table 1 summarizes the advantages and disadvantages of each approach to aid in selecting the right method depending on the application.

We chose base (NaOH) for our experiments because it removes the oxide layer and keeps the metal surface pristine in the absence of oxidative potentials. ESI[†] S4 reports the behavior of the metal in pH neutral solutions such as sodium fluoride (NaF). Cathodic potentials can direct the metal in NaF solutions in a manner similar to NaOH solutions. An electrochemical oxidative reaction occurs between the liquid metal and NaF solution upon application of a small anodic potential to the liquid metal (see Fig. S3F[†]). Without the presence of base, this oxide layer accumulates and makes the flow difficult to control.

We conducted experiments using acidic solutions such as 1 M hydrochloride (HCl), which also removes the oxide layer. CEW of EGaIn is known to be ineffective in acidic solutions,³ which is also the case here under cathodic potentials. Anodic potentials drive the electrochemical oxidation of EGaIn and thereby halt flow, but the acid is not as effective as removing the excess oxide as NaOH. For these reasons, NaOH appears to be a superior electrolyte than HCl.

Conclusion

In summary, we demonstrate a novel method for controlling the flow of liquid metal in microchannels simply by applying a modest voltage to the metal relative to a counter electrode placed in the outlet. This method directs the flow of liquid metal through complex microchannels in a manner similar to a valve but with no mechanical parts. Electrocapillarity helps direct the metal in the case of cathodic potentials, and surface oxidation of the liquid metal directs the metal in the case of anodic potentials. We demonstrate the capability of our method for directing the flow of liquid metal towards multiple outlets sequentially or simultaneously using only modest voltages, although in principle, the method may be implemented to direct flow in complex channels with multiple pathways that terminate in a single outlet. This method

for directing the flow of liquid metal may find applications in the areas of microfluidics and microelectromechanical systems (MEMS), such as reconfigurable and adjustable electronic circuits^{8–12} as well as micro-cooling systems.⁷ A drawback of this method in its current implement is the use of basic NaOH electrolytes and the tendency of the metal to break up into droplets through interfacial instabilities in some configurations.

Acknowledgements

MDD acknowledges support from the Air Force Research Lab and the NSF CAREER Award (CAREER CMMI-0954321).

References

- 1 M. D. Dickey, R. C. Chiechi, R. J. Larsen, E. A. Weiss, D. A. Weitz and G. M. Whitesides, *Adv. Funct. Mater.*, 2008, **18**, 1097–1104.
- 2 T. Liu, P. Sen and C.-J. Kim, *J. Microelectromech. Syst.*, 2012, **21**, 443–450.
- 3 S.-Y. Tang, K. Khoshmanesh, V. Sivan, P. Petersen, A. P. O'Mullane, D. Abbott, A. Mitchell and K. Kalantar-zadeh, *Proc. Natl. Acad. Sci. U. S. A.*, 2014, **111**, 3304–3309.
- 4 M. Gao and L. Gui, *Lab Chip*, 2014, **14**, 1866–1872.
- 5 J.-H. So and M. D. Dickey, *Lab Chip*, 2011, **11**, 905–911.
- 6 S.-Y. Tang, V. Sivan, P. Petersen, W. Zhang, P. D. Morrison, K. Kalantar-zadeh, A. Mitchell and K. Khoshmanesh, *Adv. Funct. Mater.*, 2014, **24**, 5851–5858.
- 7 S.-Y. Tang, J. Zhu, V. Sivan, B. Gol, R. Soffe, W. Zhang, A. Mitchell and K. Khoshmanesh, *Adv. Funct. Mater.*, 2015, **25**, 4445–4452.
- 8 J. H. So, J. Thelen, A. Qusba, G. J. Hayes, G. Lazzi and M. D. Dickey, *Adv. Funct. Mater.*, 2009, **19**, 3632–3637.
- 9 M. Kubo, X. Li, C. Kim, M. Hashimoto, B. J. Wiley, D. Ham and G. M. Whitesides, *Adv. Mater.*, 2010, **22**, 2749–2752.
- 10 R. C. Gough, A. M. Morishita, J. H. Dang, W. Hu, W. Shiroma and A. T. Ohta, *IEEE Access*, 2014, **2**, 874–882.
- 11 G. Li, M. Parmar and D.-W. Lee, *Lab Chip*, 2015, **15**, 766–775.
- 12 S. Cheng and Z. Wu, *Adv. Funct. Mater.*, 2011, **21**, 2282–2290.
- 13 S. Liu, X. Sun, O. J. Hildreth and K. Rykaczewski, *Lab Chip*, 2015, **15**, 1376–1384.
- 14 A. Fassler and C. Majidi, *Lab Chip*, 2013, **13**, 4442–4450.
- 15 N. Hallfors, A. Khan, M. D. Dickey and A. M. Taylor, *Lab Chip*, 2013, **13**, 522–526.

- 16 B. Bae, N. Kim, H. Kee, S.-H. Kim, Y. Lee, S. Lee and K. Park, *J. Microelectromech. Syst.*, 2002, **11**, 344–354.
- 17 M. M. Teymoori and E. Abbaspour-Sani, *Sens. Actuators, A*, 2005, **117**, 222–229.
- 18 T. Goettsche, J. Kohnle, M. Willmann, H. Ernst, S. Spieth, R. Tischler, S. Messner, R. Zengerle and H. Sandmaier, *Sens. Actuators, A*, 2005, **118**, 70–77.
- 19 A. Luque, J. M. Quero, C. Hibert, P. Flückiger and A. M. Gañán-Calvo, *Sens. Actuators, A*, 2005, **118**, 144–151.
- 20 H. Takao, K. Miyamura, H. Ebi, M. Ashiki, K. Sawada and M. Ishida, *Sens. Actuators, A*, 2005, **119**, 468–475.
- 21 C. Goll, W. Bacher, B. Buestgens, D. Maas, W. Menz and W. Schomburg, *J. Micromech. Microeng.*, 1996, **6**, 77.
- 22 C. Neagu, J. Gardeniers, M. Elwenspoek and J. Kelly, *Electrochim. Acta*, 1997, **42**, 3367–3373.
- 23 A. Baldi, Y. Gu, P. E. Loftness, R. A. Siegel and B. Ziaie, *J. Microelectromech. Syst.*, 2003, **12**, 613–621.
- 24 K. W. Oh and C. H. Ahn, *J. Micromech. Microeng.*, 2006, **16**, R13.
- 25 M. R. Khan, C. B. Eaker, E. F. Bowden and M. D. Dickey, *Proc. Natl. Acad. Sci. U. S. A.*, 2014, **111**, 14047–14051.
- 26 K. Kalantar-zadeh and B. Fry, *Nanotechnology-enabled sensors*, Springer Science & Business Media, 2007.
- 27 M. R. Khan, C. Trlica, J.-H. So, M. Valeri and M. D. Dickey, *ACS Appl. Mater. Interfaces*, 2014, **6**, 22467–22473.
- 28 D. C. Grahame, *Chem. Rev.*, 1947, **41**, 441–501.
- 29 G. Beni, S. Hackwood and J. L. Jackel, *Appl. Phys. Lett.*, 1982, **40**, 912–914.
- 30 R. C. Gough, A. M. Morishita, J. H. Dang, M. R. Moorefield, W. A. Shiroma and A. T. Ohta, *Micro. Nano. Syst. Lett.*, 2015, **3**, 4.